

Influence of Burner Diameter on Premixed Flame Shape and Quenching



Lateef Talab Obaid¹, Hasanain A. Abdul Wahhab², Miqdam T. Chaichan^{3*}, Mohammed A. Fayad³, Gazy F. Al-Sumaily³

¹ Manufacture of Cylinder Department, State Company for Gas Filling and Services, Ministry of Oil, Al-Kut 35048, Iraq

² Training and Workshop Center, University of Technology-Iraq, Baghdad 35050, Iraq

³ Energy and Renewable Energies Technology Center, University of Technology, Baghdad 35050, Iraq

Corresponding Author Email: miqdam.t.chaichan@uotechnology.edu.iq

Copyright: ©2023 IIETA. This article is published by IIETA and is licensed under the CC BY 4.0 license (<http://creativecommons.org/licenses/by/4.0/>).

<https://doi.org/10.18280/ijcmem.110406>

ABSTRACT

Received: 20 May 2023

Revised: 21 August 2023

Accepted: 13 September 2023

Available online: 30 December 2023

Keywords:

quenching flame, premixed counter flame, quenching diameter, burning velocity, counter burner

The quenching of a pre-mixed counter flame was studied experimentally, as described in this paper. Experimental research has been done on flames spreading in methane/air mixes in counter burners with various burner diameters. It has been determined how the counter burner diameter changes, the methane/air mixing ratio affects the flame burning velocity, and the quenching diameter. In this study, the quenching diameter was examined in relation to altering burner diameter (9, 12, 16, 19, and 23 mm) using a digital image processing technique. In counter flame, significant results were attained. The geometry of the burner edges and the air and fuel velocity have an impact on the quenching diameter in the counter flow. The top and bottom flame disc quenching diameters are nearly equal for both lean and rich combinations and grow with the burner diameter. The values of the quenching distance were smaller than the quenching diameter at the wide range of the equivalence ratio ($0.46 < \phi < 1.57$) for mixtures, and this behavior was likely caused by the dead space.

1. INTRODUCTION

Clean and efficient combustion technologies are being introduced to reduce emissions and greenhouse gases to respond to air pollution and global warming [1]. More than 60% of global warming is caused by carbon dioxide (CO₂), a primary product of hydrocarbon combustion [2]. During 2000 to 2010, greenhouse gas emissions increased by 80%, with an average annual increase of 8% [3]. Many countries worldwide have seriously promised to reduce combustion exhaust gas emissions, the major cause of air pollution and global warming. To achieve clean and efficient energy generation, combustion system designers continuously improve combustion technologies [4]. It is essential to have incinerators in energy production in many applications. Various liquid and gaseous fuels are used, including diesel, biodiesel, natural gas, liquefied petroleum gas, etc. [5, 6].

The flame spread has been the subject of many research studies focused on the design and operation of incinerators. In most combustion processes, fuels and their mixtures are premixed with air before being burned [7]. Flame spread in medium combustion can be divided into two types. As one of these two types, the flame spreads until combustion and cooling begin [8]. The other type is quenched by walls [9]. A wide range of operating conditions is required to obtain these flame states.

NOx emissions are significantly reduced when the burner is operated with a lean air-fuel mixture [10], and a significant reduction in pollutants such as CO, HC, and PM [11]. Various

burner geometries and operating conditions have been studied empirically to determine flame limits [12-14]. A clear focus was also placed on the types of fuels used and the combustion conditions. Various studies have assisted the design of combustion devices with greater stability limits. Understanding the fundamentals of difficult combustion is influenced by design and operation. This includes turbulence, kinetics, and phase changes [15, 16].

When the flame approaches the wall, its behavior changes, and combustion reactions are strongly influenced by the wall surface's specifications and temperature [17]. As a result of the heat loss, the chemical reactions are slowed, and the premixed flame stops spreading toward the wall. This extinguishes the flame front [18]. Surface conditions (temperature, material, geometry, near-surface gas dynamics, flame expansion) and combustion medium (temperature, pressure, composition) play an important role in this cooling phenomenon [19]. Burners, ramjets, pilot combustors, and other combustion tools are designed to minimize the flame-quenching phenomena [20].

The key concern for the designers was how to avoid having the flame front pushed outside of the combustion chamber or separated from the burner edge as a result of the unburned gases' high velocity as they collided with the flame. In the combustion process, quenching often refers to putting out a flame. Burners' and combustion chamber walls experience flame quenching [21]. The quenching diameter, abbreviated dq, is the minimum flame separation distance that cannot be achieved. This definition states that the quenching diameter

value depends on the fuel type, mixing ratio, and flame propagation directions (burner edge design) [22-25]. In order to comprehend the combustion process close to the burner wall, it is crucial to understand the flame quenching study by the wall [26, 27]. For premixed flames in methane/air combinations and another investigation in propane/air mixtures, the quenching diameter and flame properties escort to quenching circumstances were investigated [28-30]. Whether the flame front on the burners is facing uphill or downward determines the quenching diameter. The physical characteristics used to illustrate the differences in flame propagation properties are the ideal diffusion flame and its stretch [31-33].

In this experimental investigation, methane and air are premixed before entering the burner. The study focused on determining the influence of the changing nozzle diameter for the counter burner on the quenching diameter for propagating flames through the counter burner (disc and double disc flames) in methane/air mixtures. In this study, direct cooling distance measurements near the surface of a flame were collected using a modern, high-resolution technique. For the study of flame suppression, the optical system was used to record the stabilization disc and front images of a dual-disk flame.

2. EXPERIMENTAL SETUP

The experimental data for premixed counter flames were collected by using a combustor system, including counter ramjet and the optical technique. The wide range for disc and double disc flames are prepared; fuel gas (Methane) and air flow rates are tested. The optical system recorded the stability disc/double disc-shaped flame front images required to study quenching flame. The system components are shown in Figure 1. The counter burner includes two copper pipes at 30 mm diameter, fixed in the counter direction by steel structure, and many nozzles with different diameters: 9, 12, 16, 19, and 23 mm. The distance between burner edges was fixed at 40 mm. The current study dealt with the premixing process as the most important combustion process used in industrial furnaces, and the methane-air mixture was prepared before it reached the nozzles of the counter burner to reduce the effect of the outside air surrounding the two burner nozzles. This area was surrounded by a nitrogen container (a transparent container of heat-resistant glass filled with gas Nitrogen during burner operation). During the trials, a pair of air flowmeters was used for measuring airflow rates, while a second pair was used to assess CH₄ gas flow rates. A wide range of equivalent ratios were also investigated. The fuel/air ratios were obtained by controlling the flow rates of both petrol and air, and the equivalent ratios were calculated.

The studies employed a digital camera called the "Phantom VEO 440" with a frame rate of 180 frames per second. The optical system consists of a collection of lenses and a (He-Ne) laser source with a power of 0.21 mW and a wavelength of 713 nm. Images of the flames were captured at a resolution of 1280 720 dpi. When the camera was installed in front of the test rig at a 90° angle for the laser path, it was placed on a fixed base. When the top and bottom borders of the counter burner stayed fixed, all procedures for the optical alignment along the test rig section were confirmed. By adjusting the nozzle angles for the burner's edges and CH₄-air for a broad range of equivalency ratios (0.46 1.57), images for flame discs with

good contrast have been created. Additionally, a straightforward spark ignition system was installed close to the burner's edges to initiate mixture combustion. The geometrical properties of the flames with various nozzle sizes, the burning velocity, and the quenching diameter were calculated using flame images received from experiments. In experiments, the maximum mixture composition was incrementally approached until the flame disc's ability to move between the top and bottom burner edges was completely lost. Images taken with the digital camera demonstrated the dead area.

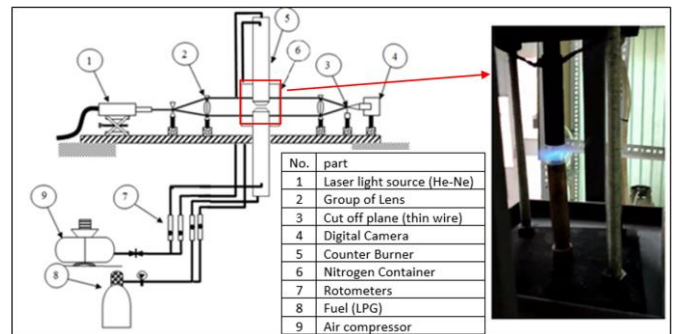


Figure 1. Schematic view of the experimental setup

A digital image processing technique was used to collect data from the recorded flame images, and a MATLAB code was developed to carry out this purpose. This algorithm is divided into three steps: flame front determination, flame attributes collection, and calculation of flame parameters. Figure 2 shows the algorithm structure and main flame parameters. The first stage included the noise reduction in the flame image background by subtraction it from the source image. In order to produce a flame front image with less background noise, a calibration image (source image) was obtained without combustion and compared to each image. The original image was converted into a binary image in the second stage using a threshold ratio of roughly 0.8-0.85. The thresholding process results in a binary image calibrating an actual value or threshold to the matrix pixel numbers, consequently, it assigns the value 1 (white) to all pixels in the chosen image with contrast above a threshold and the value 0 (black) to all other pixels. More so, several morphological operations were used to improve the quality of the binary image, such as the erosion and dilation method and speckle reduced by using an opening operation. The third stage includes quantitative analysis of the flame front in images and measuring several parameters; flame spatial location, disc, double disc flame diameter, burning velocity, and the flame quenching diameter. According to the most popular approach, the burning velocity was calculated by measuring the amount of gas mixture consumed per second and dividing it by the flame disc's surface area [12].

$$Su = \frac{4Q_{mix}}{\pi \cdot d_c^2} \quad (1)$$

where, Su is the burning velocity cm/s, d_c is flame disc diameter (mm), Q_{mix} is unburned gases volumetric flow (cm³/s). Also, the main parameter for determining the quenching diameter is the critical Peclet number (Pe) and the flammability of the combustion mixture [30].

$$Pe = \frac{Su \cdot d}{\eta} \quad (2)$$

where, η is the thermal diffusivity of the unburned mixture, and d is the flame-quenching diameter.

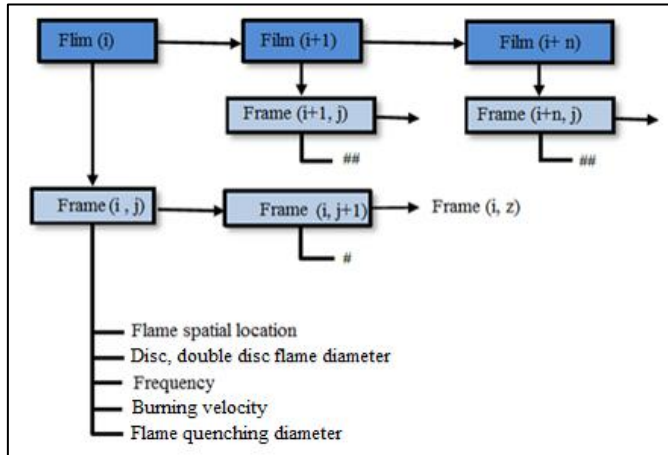


Figure 2. The flame structure data and main parameters in digital image processing

3. RESULTS AND DISCUSSION

The counter flame photos for a wide variety of equivalency ratios in the various burner diameters-9, 12, 16, 19, and 23 mm-were first captured during the experiments. To analyse the behaviour of the counter flame when it propagates in them, their diameters were thus gradually raised. Figure 3 displays the Su burning velocities and a function of the equivalency ratio for rich and lean sides for methane/air mixture at various nozzle orientations. According to the statistics, the burning velocity increased with increasing nozzle diameter.

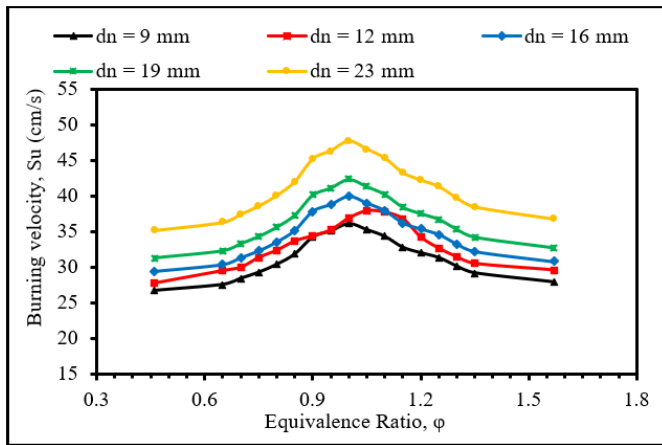


Figure 3. Burning velocity as a function of the equivalence ratio for a different nozzle diameter

The counter burner's nozzle diameter has a less significant impact on the Su flame-burning velocity, as demonstrated in Figure 4. For nozzle diameters greater than 12 mm, the nozzle angle of the burner also has a similar impact on the rate of flame propagation. For higher levels of these parameters, a difference in flame propagation velocity is apparent. For a stoichiometric mixture, the burning velocity in a nozzle with a

diameter of 9 mm is lower than in nozzles with higher diameters.

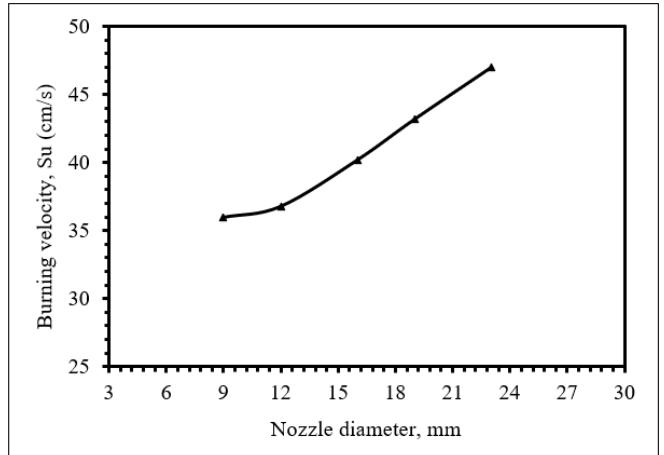


Figure 4. Burning velocity as a function of the nozzle diameter for a stoichiometric mixture

For narrower nozzle edges, the cooling effect of the burner edges on the flame is noticeable. The relationship between the dead space and nozzle diameter ratio and this effect is depicted in Figure 5 (changing nozzle diameter is dependent on increasing nozzle angle). With the nozzle diameter lowering up to 9 mm, the dead space and nozzle diameter ratio marginally rise. This rise is more pronounced and more frequently accompanied by a decline in laminar burning velocity and a potential reduction in the local temperature of a chemical reaction for smaller nozzle sizes. On the other hand, the bottom flame disc had a higher dead space to nozzle diameter ratio at a modest nozzle diameter of 9 mm than the top disc flame.

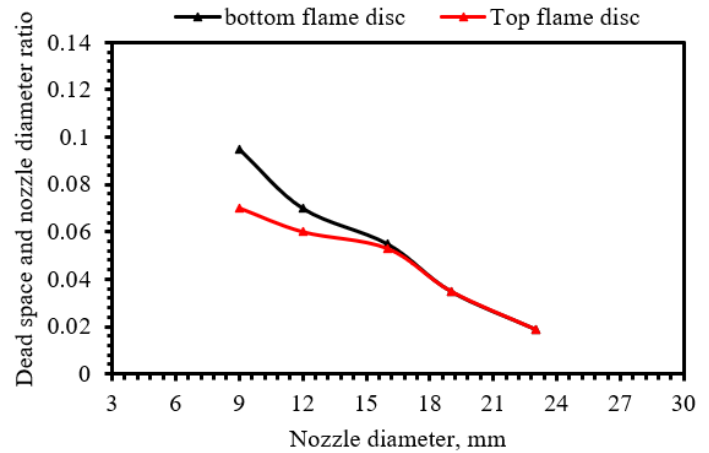


Figure 5. Dead space and nozzle diameter ratio as a function of burner diameter

Figure 6 shows variations between the propagation limits of the disc and double disc counter flames in lean and rich mixes with nozzle diameter=16 mm based on photos captured by the digital camera. Generally, there are many differences in the color of the flame front with the dead space, so lean mixtures for either flame disc or double disc were blue, while the rich ones show a bright blue. Figure 7 displays the quenching diameters as a function of mixture concentration. For lean and rich mixes, the quenching diameters nearly always rise as the nozzle diameter does. Additionally, due to dead space, the

quenching diameter values for all combinations within the equivalence ratios were higher than the quenching distance.

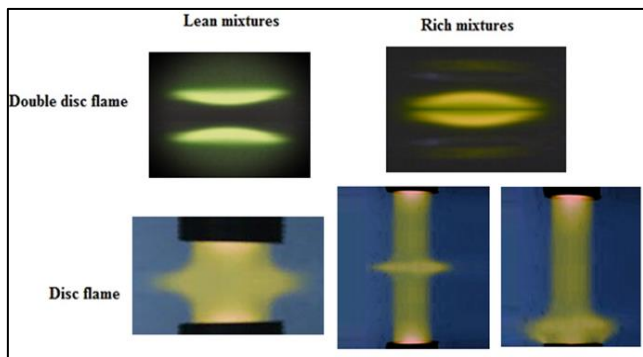


Figure 6. Images of the disc and double disc flames for lean and rich mixtures

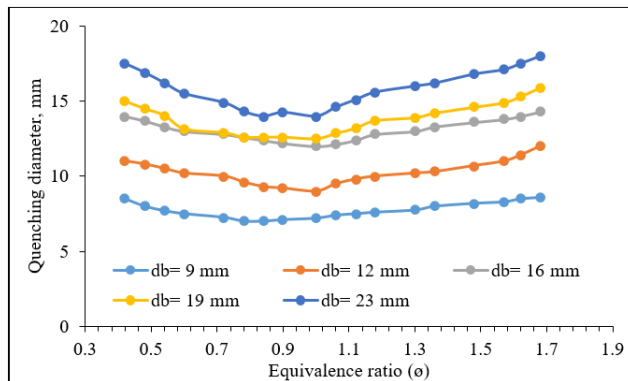


Figure 7. Experimentally determined quenching diameter as a function of the equivalence ratio

Figure 8 shows the comparison between experimental measurement results and experimental results in the literature of the burning velocity at 19 mm burner diameter shows a good agreement in the premixed flames. The mean percentage of differences between the literature results of premixed flame and the experimental measurement is 8.8%.

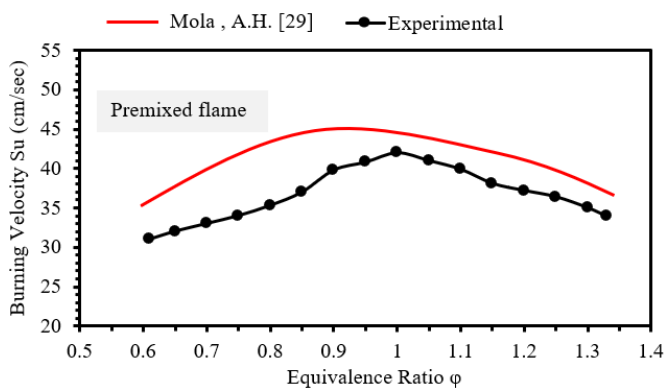


Figure 8. V of burning velocity at burner diameter 19 mm

4. CONCLUSIONS

The analysis of multiple experimental findings presented in this study enables consideration of potential quenching limits for premixed counter flames. Experimental research has been done on flames in methane/air mixes propagating in the

counter burner at various nozzle angles. It has been calculated how the counter burner's nozzle angles change with the methane/air mixing ratio, flame burning velocity, and quenching diameter. In this study, the quenching diameter was examined in relation to altering burner diameter (9, 12, 16, 19, and 23 mm) using a digital image processing technique. The findings for the flaming disc and double disc were obtained within the stability bounds. Basically, the diameter of the nozzle and the velocity of the fuel/air mixture determine the quenching diameter for the counter burner. The quenching diameters for the top and bottom flame discs are nearly identical for both lean and rich mixtures, and they become larger with nozzle diameter. All mixtures within the equivalence ratios ($0.46 < \phi < 1.57$) had quenching diameter values greater than quenching distance due to the existence of dead space.

ACKNOWLEDGMENTS

The authors are obliged to the University of Technology, Baghdad, for providing the center for automotive and energy generation.

REFERENCES

- [1] Dhahad, H.A., Chaichan, M.T., Megaritis, T. (2019). Performance, regulated and unregulated exhaust emission of a stationary compression ignition engine fueled by water-ULSD emulsion. Energy, 181: 1036-1050. <https://doi.org/10.1016/j.energy.2019.05.200>
- [2] Tran, N., Ta, Q.T.H., Nguyen, P.K.T. (2022). Transformation of carbon dioxide, a greenhouse gas, into useful components and reducing global warming: A comprehensive review. International Journal of Energy Research, 46(13): 17926-17951. <https://doi.org/10.1002/er.8479>
- [3] Olivier, J.G., Schure, K.M., Peters, J.A.H.W. (2017). Trends in global CO₂ and total greenhouse gas emissions. PBL Netherlands Environmental Assessment Agency, 5: 1-11.
- [4] Ağbulut, Ü., Sarıdemir, S. (2021). A general view to converting fossil fuels to cleaner energy source by adding nanoparticles. International Journal of Ambient Energy, 42(13): 1569-1574. <https://doi.org/10.1080/01430750.2018.1563822>
- [5] Chaichan, M.T. (2018). Combustion and emission characteristics of E85 and diesel blend in conventional diesel engine operating in PPCI mode. Thermal Science and Engineering Progress, 7: 45-53. <https://doi.org/10.1016/j.tsep.2018.04.013>
- [6] Ekaab, N.S., Hamza, N.H., Chaichan, M.T. (2019). Performance and emitted pollutants assessment of diesel engine fuelled with biokerosene. Case Studies in Thermal Engineering, 13: 100381. <https://doi.org/10.1016/j.csite.2018.100381>
- [7] Wang, G., Tang, P., Li, Y., Xu, J., Durst, F. (2019). Flame front stability of low calorific fuel gas combustion with preheated air in a porous burner. Energy, 170: 1279-1288. <https://doi.org/10.1016/j.energy.2018.12.128>
- [8] Wang, G., Shi, Z., Xu, G., Luo, D., Xu, J. (2022). Experimental study on the combustion of low-calorific NG/N₂ in a porous burner. Energy Science &

- Engineering, 10(4): 1202-1213. <https://doi.org/10.1002/ese3.1095>
- [9] El Hadi Attia, M., Chaichan, M.T., Driss, Z. (2022). Study characterization of the methane flame enriched with hydrogen or nitrogen. AIP Conference Proceedings, 2415: 020016. <https://doi.org/10.1063/5.0092299>
- [10] Zarei, R., & Emami, M. D. (2022). Development of an air/fuel premixer for a gas-fueled two-layer porous media burner. Combustion Science and Technology, Latest Articles. <https://doi.org/10.1080/00102202.2022.2086801>
- [11] Attia, M.E.H., Rout, S.K., Hussein, A.K., Chaichan, M. T., Ghodbane, M., Ali, H.M., Driss, Z. (2020). CFD simulation of the Co emissions of pollutants contained in flames H₂-C₃H₈/Air. In 2020 International Conference on Renewable Energy Integration into Smart Grids: A Multidisciplinary Approach to Technology Modelling and Simulation (ICREISG), Bhubaneswar, India, pp. 222-227. <https://doi.org/10.1109/ICREISG49226.2020.9174541>
- [12] Mutlu, K., & Taştan, M. (2023). Investigation of combustion instability of propane fuel enriched with oxygen under acoustic enforcement. Petroleum Science and Technology, Research Article. <https://doi.org/10.1080/10916466.2023.2191639>
- [13] Attia, M.E.H., Chaichan, M.T., Driss, Z., Khechekhouche, A. (2020). Computer simulation of CH₄-G222-H₂ behaviour in a non-premixed combustion chamber. Thermal Science and Engineering Progress, 17: 100389. <https://doi.org/10.1016/j.tsep.2019.100389>
- [14] Lamioni, R., Bronzoni, C., Folli, M., Tognotti, L., Galletti, C. (2023). Effect of slit pattern on the structure of premixed flames issuing from perforated burners in domestic condensing boilers. Combustion Theory and Modelling, 27(2): 218-243. <https://doi.org/10.1080/13647830.2022.2157753>
- [15] Lu, Y., Xiao, Y., Wu, J., Chen, L. (2022). Nonlinear combustion instability analysis of a bluff body burner based on the flame describing function. Proceedings of the Institution of Mechanical Engineers, Part G: Journal of Aerospace Engineering, 236(9): 1751-1765. <https://doi.org/10.1177/09544100211044021>
- [16] Wu, W., Liu, J., Guo, S., Zeng, Z., Cui, G., Yang, Z. (2022). Optimization research on burner arrangement of landfill leachate concentrate incinerator based on “3T+E” principle. Energies, 15(16): 5855. <https://doi.org/10.3390/en15165855>
- [17] Plathner, F.V., Quintiere, J.G., van Hees, P. (2019). Analysis of extinction and sustained ignition. Fire Safety Journal, 105: 51-61. <https://doi.org/10.1016/j.firesaf.2019.02.003>
- [18] Pradhan, A., Pattnaik, S., Bastia, A.A., Samantray, S. (2023). Combustion characteristic and optimization of round jet burner using Syngas. Materials Today: Proceedings, 80: 219-225. <https://doi.org/10.1016/j.matpr.2022.12.077>
- [19] Xie, B., Peng, Q., Shi, Z., Wei, J., Kang, Z., Wei, D., Tian, X., Fu, G. (2023). Investigation of CH₄ and porous media addition on thermal and working performance in premixed H₂/air combustion for micro thermophovoltaic. Fuel, 339: 127444. <https://doi.org/10.1016/j.fuel.2023.127444>
- [20] Song, Z.B., Ding, X. W., Yu, J.L., Chen, Y.Z. (2006). Propagation and quenching of premixed flames in narrow channels. Combustion, Explosion and Shock Waves, 42: 268-276. <https://doi.org/10.1007/s10573-006-0050-6>
- [21] Kim, N.I., Maruta, K. (2006). A numerical study on propagation of premixed flames in small tubes. Combustion and flame, 146(1-2): 283-301. <https://doi.org/10.1016/j.combustflame.2006.03.004>
- [22] Abdul Wahhab, H.A., Aziz, A.R.A., El-adawy, M., Ismael, M.A., Firmansyah. (2018). Effect of rotating burner rim on flame stabilisation: Blow-off and flash back. International Journal of Engineering and Technology, 7: 230-233. <https://doi.org/10.14419/ijet.v7i3.17.21913>
- [23] Wahhab, H.A. (2021). Investigation of stability limits of a premixed counter flame. International Journal of Automotive and Mechanical Engineering, 18(1): 8540-8549. <https://doi.org/10.15282/ijame.18.1.2021.13.0648>
- [24] Zamashchikov, V.V. (2004). Some features of gas-flame propagation in narrow tubes. Combustion, Explosion and Shock Waves, 40: 545-552. <https://doi.org/10.1023/B:CESW.0000041406.83951.ca>
- [25] Maruta, K., Kataoka, T., Kim, N.I., Minaev, S., Furstenko, R. (2005). Characteristics of combustion in a narrow channel with a temperature gradient. Proceedings of the Combustion Institute, 30(2): 2429-2436. <https://doi.org/10.1016/j.proci.2004.08.245>
- [26] Jarosinski, J., Podfilipski, J., Fodemski, T. (2002). Properties of flames propagating in propane-air mixtures near flammability and quenching limits. Combustion science and technology, 174(1): 167-187. <https://doi.org/10.1080/713712915>
- [27] Law, C.K. (2010). Combustion Physics. Cambridge University Press.
- [28] Sotton, J., Boust, B., Labuda, S.A., Bellenoue, M. (2005). Head-on quenching of transient laminar flame: heat flux and quenching distance measurements. Combustion science and technology, 177(7): 1305-1322. <https://doi.org/10.1080/0010220059050485>
- [29] Mola, A.H., Abdul Wahhab, H.A., Naji, Z.H. (2022). Effects of nozzle diameter and number of carbon atoms in fuel on flame quenching in counter burner. In ICPER 2020: Proceedings of the 7th International Conference on Production, Energy and Reliability, pp. 123-131. https://doi.org/10.1007/978-981-19-1939-8_11
- [30] Abdul wahhab, H.A. (2022). Influence of swirl flow pattern in single tube burner on turbulent flame blow-off limit. In ICPER 2020: Proceedings of the 7th International Conference on Production, Energy and Reliability, pp. 17-34. https://doi.org/10.1007/978-981-19-1939-8_2
- [31] Bellenoue, M., Kageyama, T., Labuda, S.A., Sotton, J. (2003). Direct measurement of laminar flame quenching distance in a closed vessel. Experimental Thermal and Fluid Science, 27(3): 323-331. [https://doi.org/10.1016/S0894-1777\(02\)00304-7](https://doi.org/10.1016/S0894-1777(02)00304-7)
- [32] Sher, E., Heywood, J.B., Hacohen, J. (1992). Heat transfer to the electrodes a possible explanation of misfire in SI-engines. Combustion Science and Technology, 83(4-6): 323-325. <https://doi.org/10.1080/00102209208951839>
- [33] Karrer, M., Labuda, S., Sotton, J., Bellenoue, M. (2009). Experimental study of single wall flame quenching at high pressures. In 22th International Colloquium on

Greek symbols

η The thermal diffusivity

NOMENCLATURE

d_q Quenching diameter, in [mm]
 d_c Disc flame diameter, in [mm]